Installing Lactone Chain Termini During Photoinduced Polymerization

Journal:	*Polymer Chemistry*
Manuscript ID	PY-COM-03-2018-000457.R1
Article Type:	Communication
Date Submitted by the Author:	07-Apr-2018
Complete List of Authors:	Lauer, Andrea; Karlsruhe Institute of Technology, Institute of Technical and Polymer Chemistry Steinkönig, Jan; Karlsruhe Institute of Technology, Institute of Chemical Technology and Polymer Chemistry; Institut of Biological Interfaces, Jöckle, Philipp; Karlsruhe Institute of Technology, Institut für Physikalische Chemie Kelterer, Anne-Marie; Graz University of Technology, Institute of Physical and Theoretical Chemistry Unterreiner, Andreas; Karlsruhe Institute of Technology, Physical Chemistry Barner-Kowollik, Christopher; Queensland Universtiy of Technology, School of Chemistry, Physics and Mechanical Engineering; Karlsruhe Institute of Technology, Institut für Technische Chemie und Polymerchemie

Polymer Chemistry

COMMUNICATION

Installing Lactone Chain Termini During Photoinduced Polymerization

Received 00th January 20xx,
Accepted 00th January 20xx

DOI: 10.1039/x0xx00000x

www.rsc.org/

Andrea Lauer,[a,b,c,†] Jan Steinkoenig,[a,b,c,†] Philipp Jöckle,[a,b,c,e] Anne M. Kelterer,[d,*] Andreas N. Unterreiner,[e,*] and Christopher Barner-Kowollik[a,b,c,*]

We exploit the Thorpe-Ingold effect as a spontaneous end group transformation method during photo-induced polymerization of methacrylates using the functional (2-hydroxy-4´-(2-hydroxyethoxy)-2-methylpropio-phenone) species as radical photoinitiator. Herein, the isopropyl hydroxyl function endows the polymer with geminal methyl groups inducing an angular compression, enabling through close proximity a ring-closing reaction between the hydroxyl group and the ester motif.

Photoinduced polymerization is an attractive and versatile technique to fabricate and process materials. Substantial research efforts are directed at shifting the absorbance spectrum of photoreactive compounds, including photoinitiators (PIs), from the UV light regime to visible light[1,2] and to establish λ-orthogonal photochemistry for precision photoresist design for 3D laser lithography.[3,4,5,6,7] Among the most important photochemically reactive molecules, radical generating photoinitiators are critical for a wide range of applications in industry from 3D printing,[8,9] photo curing of coatings,[10,11] dental restorative materials,[12] photoresists[13] to ink technology.[14] The structural motives entailed in radical photoinitiators lead to either a Norrish Type I or Type II cleavage. Type I initiators generate a radical in a unimolecular process via α-cleavage. Type II initiators induce a proton or electron abstraction of donor molecules – which subsequently starts the polymerization – after being transitioned to an excited electronic state. Most prominent candidates are hydroxyalkylphenones,[15,16] acylphosphine oxides,[17,18] and acylgermanes[19,20] (Type I initiator) as well as thioxanthones[21,22] and benzophenones[23,24] (Type II initiator). Associated with their characteristic cleavage mechanism, the radical initiator fragments inducing the polymerization are found in the polymer as distinct end group motifs. Importantly, depending on the structural nature of a Type I initiator, one of both fragments can quantitatively dominate as chain terminus. Thus, the precision determination of end groups in photoinitiation processes[25,26] is of fundamental importance, especially if the end group is endowed with functionalities allowing for post-polymerization modifications.[27]

One example of a highly functional photoinitiator is Irgacure 2959 (2-hydroxy-4´-(2-hydroxyethoxy)-2-methylpropio-phenone), which can be activated at 351 nm with subsequent radical release in a Norrish Type I reaction. Although Irgacure 2959 generates two structurally different radical fragments, i.e. an isopropyl alcohol radical and a hydroxyethoxy-phenylcarbonyl radical, both entail hydroxyl motifs for further functionalization.[28]

In 1915, Beesley, Thorpe and Ingold[29] discovered that geminal substitution (e.g. two methyl groups) accelerates cyclization reactions, termed the Thorpe-Ingold effect.[30,31] Interestingly, an isopropyl alcohol chain terminus as generated by Irgacure 2959 equips the polymer with geminal methyl groups introducing an angular compression of the tetrahedral end group center. Thus, the methyl groups lock the free rotation and the angle compression forces adjacent functional moieties to react, forming a cyclic structure.

Despite its broad application in fundamental research and a wide array of industrial applications, it is surprising that the polymer chains and the chain termini generated by Irgacure 2959 have never been subjected to an in-depth high resolution mass spectrometric investigation, including the proposed Thorpe-Ingold effect affording lactones as end groups.

Herein, we close this critical analytical gap, which greatly influences the use of the initiator. During the spontaneous

[a.] *School of Chemistry, Physics and Mechanical Engineering, Queensland University of Technology (QUT), 2 George Street, QLD 4000, Brisbane, Australia, christopher.barnerkowollik@qut.edu.au*
[b.] *Macromolecular Architectures, Institut für Technische Chemie und Polymerchemie, Karlsruhe Institute of Technology (KIT), Engesserstr. 18, 76131 Karlsruhe, Germany, christopher.barner-kowollik@kit.edu*
[c.] *Institut für Biologische Grenzflächen (IBG), Karlsruhe Institute of Technology (KIT), Herrmann-von-Helmholtz-Platz 1, 76344 Eggenstein-Leopoldshafen, Germany*
[d.] *Institute of Physical and Theoretical Chemistry, NAWI Graz, Graz University of Technology, Stremayrgasse 9, 8010 Graz, Austria, kelterer@tugraz.at*
[e.] *Molekulare Physikalische Chemie, Institut für Physikalische Chemie, Karlsruhe Institute of Technology (KIT), Fritz-Haber-Weg 2, 76131 Karlsruhe, Germany*
† These authors contributed equally, andreas.unterreiner@kit.edu
Electronic Supplementary Information (ESI) available: [details of any supplementary information

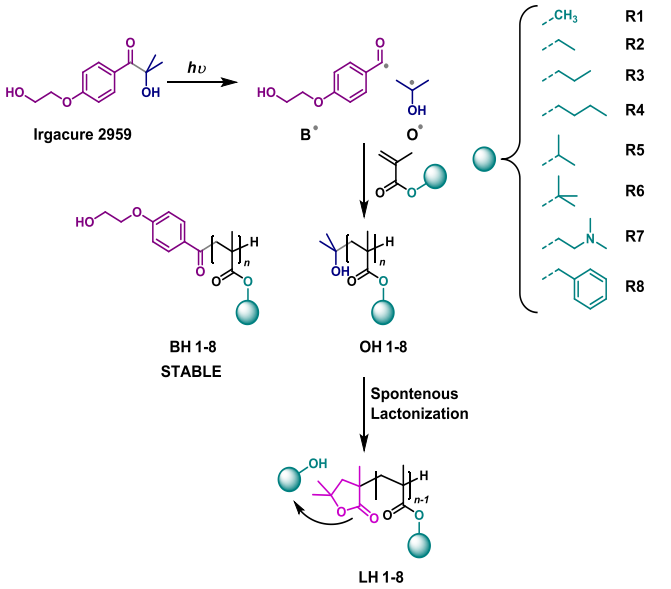

Scheme 1 End Group Transformations of Photochemically Generated (Irgacure 2959) Hydroxy Isopropyl-Terminated (**OH**) Poly(methacrylates, R1-R8), Induced by the Trimethyl-Lock Effect to Obtain Lactone-Derived End Groups (**LH**).

lactonization, the alcohol of the methyl methacrylic ester is expelled. We hypothesize that the cyclization kinetics are a function of the monomer's ester moiety, the irradiation wavelength, the reaction temperature and the irradiation intensity. Thus, pulsed-laser polymerization, using a wavelength-tunable monochromatic laser system and an excimer-laser system operating at the XeF line (λ = 351 nm) – which enables high energies and in our configuration a variable temperatures sample holder – combined with size exclusion chromatography hyphenated with high resolution electrospray ionization-mass spectrometry (PLP-SEC-ESI-MS) was employed for the photochemical synthesis and analysis of the polymeric material. The formation of the lactone species was further underpinned by MS/MS experiments. The mechanistic pathways were additionally confirmed by PLP experiments employing a photoinitiator without the hydroxyl group (Irgacure 907).

Our detailed mass spectrometric investigation of the polymer end group patterns generated by the photoinitiator **Irgacure 2959** focusing on the Thorpe-Ingold effect induced lactonization during PLP, entails varying the monomer type (methyl methacrylate (MMA), ethyl methacrylate (EMA), *n*-propyl methacrylate (*n*PMA), *iso*-propyl methacrylate (*i*PMA), *n*-butyl methacrylate (*n*BMA), *tert*-butyl methacrylate (*t*BMA), dimethyl-amino-ethyl methacrylate (DMAEMA), and benzyl methacrylate (BnMA), the wavelength (275-360 nm), photon energy (0.7-2.5 mJ/pulse) and reaction temperature (0-60 °C). Thus, Irgacure 2959 was irradiated with pulsed UV laser light in the presence of the respective monomer, generating the radical-types denoted **B** and **OH**, both able to initiate macromolecular growth (refer to **Scheme 1**). The resulting polymers **OH 1-8** showed a spontaneous (partial) lactonization, affording the polymers **LH 1-8**, while the polymers **BH 1-8** remained unchanged. Below, we will discuss the end group formation processes based on *n*PMA to avoid repetitive mass spectrometric evaluation. All mass spectra and their complete quantitative evaluation of p(MMA), p(EMA), p(*i*PMA), p(*n*BMA), p(*t*BMA), p(DMAEMA), and p(BnMA) can be found in the Supporting Information (refer to **Figures S13-20**). Initially, **Irgacure 2959** was utilized to polymerize *n*PMA in bulk via PLP at low laser energies (0.35 mJ/pulse, λ = 351 nm, 100 Hz) to ensure intact end groups[32] and short polymer chains for subsequent mass spectrometric analysis. The residual monomer was evaporated and the polymer was analyzed via SEC-ESI-MS without further purification. The following nomenclature was employed to address the observed SEC-ESI-MS signals. Disproportionation peaks are labeled as XH^D or $X{=}^D$ and combination products as $X2^C$, where X defines the photoinitiator derived end group within the polymer chain in α-position and 2 implies that the fragment is present twice. The superscripts D and C indicate the respective disproportionation or combination products. Disproportionation peaks occur in pairs with a mass difference of 2 *m*/*z*. Thus, the end group in ω-position of the polymer chain is labeled as = (carrying a double bond) or H (saturated). Only the disproportionation products (XH) are discussed to simplify the data illustration. **Figure 1A**

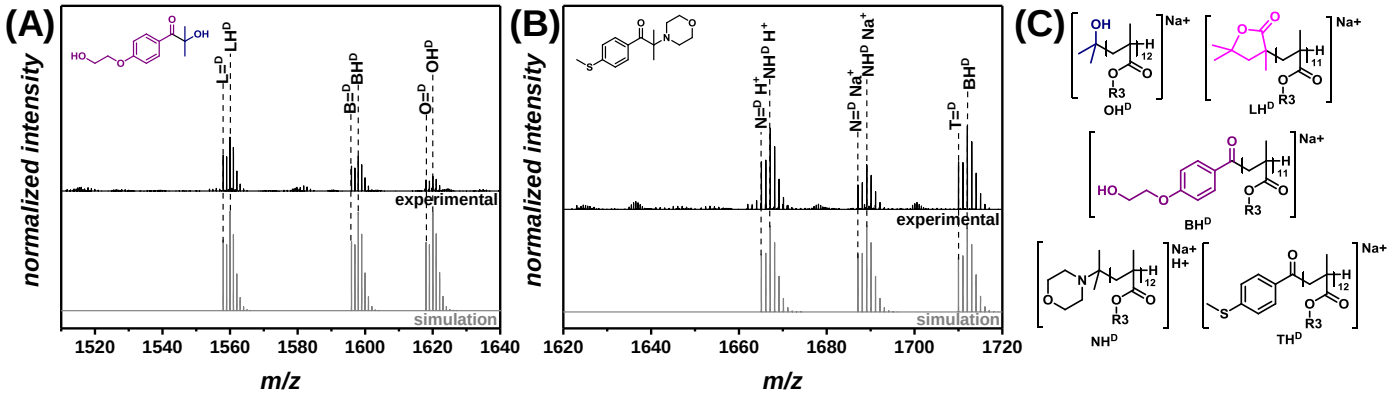

Figure 1 (**A**) High-resolution SEC-ESI mass spectra of p(*n*PMA) initiated by **Irgacure 2959**, synthesized at low laser energies (0.35 mJ/pulse, 100 Hz, 351 nm, black spectrum) and the associated isotopic pattern simulation (gray spectrum). (**B**) High-resolution SEC-ESI mass spectra of p(*n*PMA) initiated by **Irgacure 907**, synthesized at low laser energies (0.35 mJ/pulse, 100 Hz, 351 nm, black spectrum) and the corresponding isotopic pattern simulation (gray spectrum). (**C**) Disproportionation products (XH) of the polymers initiated by **Irgacure 2959** and **Irgacure 907**, at low laser energies (0.35 mJ/pulse, 100 Hz, 351 nm), as detected by SEC-ESI-MS.

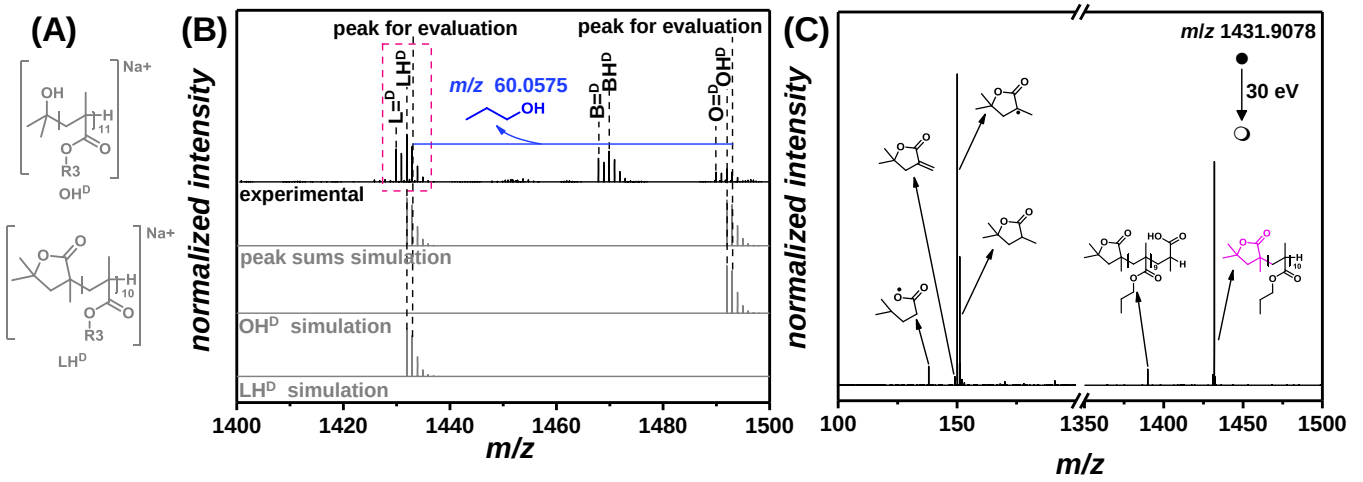

Figure 2 (A) Structure of the disproportionation products (**OH^{D}** and **LH^{D}**). (B) High-resolution SEC-ESI mass spectra of p(*n*PMA) initiated by **Irgacure 2959** at low laser energies (100 Hz, 351 nm, 0.35 mJ/pulse, black spectrum), and the theoretical isotopic pattern of **OH^{D}** and **LH^{D}**, as well as the sum of the simulation patterns (gray spectrum). (C) HCD measurements of **LH^{D}**.

depicts the high-resolution mass spectra of p(*n*PMA) initiated by **Irgacure 2959** (λ = 351 nm, 0.35 mJ/pulse, black spectrum), the associated isotopic pattern simulation (gray spectrum) and the assigned polymer structures. The experimental and theoretical *m/z* values are collated in **Table S4**. The experimental mass spectrum exhibits the expected disproportionation pattern originating from the cleavage of the photoinitiator (**B=^{D}**, **BH^{D}**, **O=^{D}**, **OH^{D}**; for the complete polymer structures refer to **Figure S5** and **Scheme S4**) and a third disproportionation pattern with signals at 1558.0 and 1560.0 *m/z* (values are taken from the mass spectrum of polymer formed via irradiation at 351 nm). ESI MS data can be biased (causing the preferred ionization of a species over another) by their ionization mainly as a result of charge competition,[33] energy required to exit the solvent shell,[34] and dipol-ion interactions.[35] The following data were acquired with constant settings of the mass spectrometer, minimizing the ionization bias to a minimum. Excluding adduct formation in positive ion mode (i.e. H^+ or K^+ attachment) of the expected **Irgacure 2959**-derived species, the additional unknown species is associated with the expected transformation of the hydroxyl isopropyl end group to a lactone terminus during PLP. Thus, species associated with the spontaneous lactone formation in case of p(*n*PMA) (labeled as **LH^{D}** and **L=^{D}**) have the highest ion abundance. The trend is consistent throughout every repeating unit of the polymer.

To confirm the presence of the lactone species in the polymer, higher-energy collision dissociation type (HCD, see **Figure 2C**) as well as ^{13}C NMR measurements were carried out. Both methods verify the presence of the lactone end group in p(*n*PMA) (for the complete ^{13}C NMR spectra refer to **Figure S21**). Importantly, we confirmed the mechanistic pathway of the lactonization by using a photoinitiator without the hydroxyl group at the isopropyl moiety. 2-methyl-4´-(methylthio)-2-morpholinopropiophenone (**Irgacure 907**) belongs to the class of the α-aminoacetophenone photoinitiators (type I PI) that cleaves into two radicals: a benzoyl- and N-isopropyl morpholino-radical. **Irgacure 907** was utilized to polymerize *n*PMA in bulk via PLP and further analyzed with SEC-ESI-MS, applying the same conditions used during PLP of **Irgacure 2959**. The absence of the cleaved alcohol ($\Delta m/z$ = 60.0575) in the mass spectra of the generated polymers shown in **Figure 1B** demonstrates that without the hydroxyl group tethered to the isopropyl moiety, the ester cannot be cleaved as no nucleophile is in direct proximity.

Critically, a quantitative comparison of the lactone species with the hydroxyl isopropyl species for every polymer initiated by **Irgacure 2959** was performed. Therefore, a method that evaluates the peak heights, Δh, of the polymer signals in each repeating unit was established. Specifically, the second peak of the respective disproportionation peak clusters (**OH** and **LH**) was selected and compared with each other (refer to **Figure 2A** and **B**). The particular peak height Δh(XH) was employed for the calculation of the ratio of χ^{XH}(i), where X defines the respective end group of the initiating or decomposition fragment (see **Eq. 1**). A plot of the χ^{XH}(i) values for each fragment XH against the degree of polymerization DP_n (see **Figure S14-17**), exhibits a constant gradient close to zero, indicating a chain length independent ionization process during SEC-ESI-MS.

$$(eq.\,1) \qquad \chi^{\mathrm{LH^D}}(n) = \frac{\Delta h^{\mathrm{LH^D}}(n)}{\Delta h^{\mathrm{LH^D}}(n) + \Delta h^{\mathrm{OH^D}}(n+1)}$$

Table 1 depicts the calculated ratios of lactonization for each polymer. The number of pulses have been selected such as sufficient polymer could be obtained while concomitantly avoiding the gel effect. Interestingly, experimentally, it can be clearly seen that the lactonization reaction occurs mainly for the polymers p(*n*PMA) (close to 80%), p(DMAEMA) (100%), and p(BnMA) (close to 85%). The polymers p(MMA), p(EMA), p(*i*PMA), p(BMA), and p(*t*BMA) presented the lactonization products as well, however, the ion abundances were low.

In order to obtain further insight into the spontaneous lactonization mechanism, detailed Density Functional Theory

Table 1 Overview of the averaged ratios of lactone end groups of the polymers, synthesized at low laser energies (351 nm, 0.35 mJ/pulse, 100 Hz) and initiated by **Irgacure 2959**, as detected by SEC-ESI-MS with a resolution of 50000. χ was calculated according to equation 1.

polymers	pulses	χLH^D	χOH^D
p(MMA)	90 000	0.10	0.90
p(EMA)	90 000	0.06	0.94
p(*n*PMA)	90 000	0.78	0.22
p(*i*PMA)	90 000	0.04	0.96
p(*n*BMA)	90 000	0.06	0.94
p(*t*BMA)	90 000	0.02	0.98
p(DMAEMA)	45 000	1.00	0.00
p(BnMA)	22 500	0.83	0.17

(DFT) calculations were performed on the reaction mechanism of **Scheme 1** including ring closure on **OH** and release of the alcohol to receive **LH**. We opted for **R3** (propyl) and **R4** (butyl) ester motifs and calculated the relative Gibbs Free energy of the reaction pathways. The nucleophilic attack of the isopropyl alcohol to the prochiral ester motif generates a chiral intermediate, which will subsequently form the lactone and liberate the propyl alcohol (or butyl alcohol). In Hanson's nomenclature, such an attack is referred to as *si* face attack (generating a *S* enantiotop) or *re* face attack (generating a *R* enantiotop).[36] The calculations showed that the *S* enantiotop is thermodynamically much more stable for both **R3** and **R4** (-54 kJ·mol^{-1} compared to the *R* enantiotop, respectively). From the thermodynamic point of view, only the *S* enantiotop of the polymer is experimentally accessible. The DFT pathway after *si* attack is presented in **Figure 3**. For completeness, the lactonization reaction after *re* attack can be found in the Supporting Information (**Table S14**, **Figure S22**).

Direct ring closure of the open polymer to the intermediate structure (see reaction in **Scheme S11**) is the rate limiting step and has a similar barrier for both substituents (153.7 kJ·mol^{-1} (**R3**) and 155.4 kJ·mol^{-1} (**R4**), respectively). In the transition state, the O-C bond length is ~1.72 Å and the proton is located between the two oxygen atoms. From this intermediate, the alcohol is released and a stable lactone-alcohol adduct was found with a lactone-alcohol distance of approximately 3.5 Å. This lactone product is thermodynamically disfavored for **R4** (+2.2 kJ·mol^{-1} over the open polymer end group), whereas for **R3** it is stabilized by -12 kJ·mol^{-1}. Thus, our DFT results confirm the experimental finding that the lactone is formed for propyl with a high ratio, but not for butyl substituents (refer to **Table 1**).

As p(*n*PMA) displays high lactone ion abundancies, a precision wavelength screen was carried out. Thus, we are able to quantify the degree of end group transformation as a function of wavelength, utilizing **Eq. 1**. **Figure 4A** depicts the high-resolution SEC-ESI-MS spectra of p(*n*PMA) initiated by **Irgacure 2959** utilizing wavelengths in the range of 275 – 360 nm, applying a constant photon count per wavelength (colored spectra). The assigned polymer structures are shown in **Figure 1C** and the experimental and theoretical *m/z*-values are collated in **Table S6**. The mass spectra of all photo-initiated polymers employing different wavelengths display the same expected disproportionation products (**L=, LH, O=, OH, B=, BH**) as it is the case for PLP at 351 nm (refer to **Figure 1A**, black spectrum). The ratio of lactonization of the polymer is invariant to the wavelength as evident from **Figure 4B**. The reduced ratio of lactonization at 275 nm (absorption maximum of Irgacure 2959) is attributed to ring-opening of the lactone during harsh irradiation conditions (refer to **Figure S13**, **Scheme S10**, **Table S10**).

Furthermore, the temperature- and energy-dependent lactonization of *n*PMA during PLP was studied and the ratio of the lactonization reaction of **Irgacure 2959-p(*n*PMA)**, derived from the peak height **Δ*h*(LH^D)** are depicted in **Table S13-14**. The

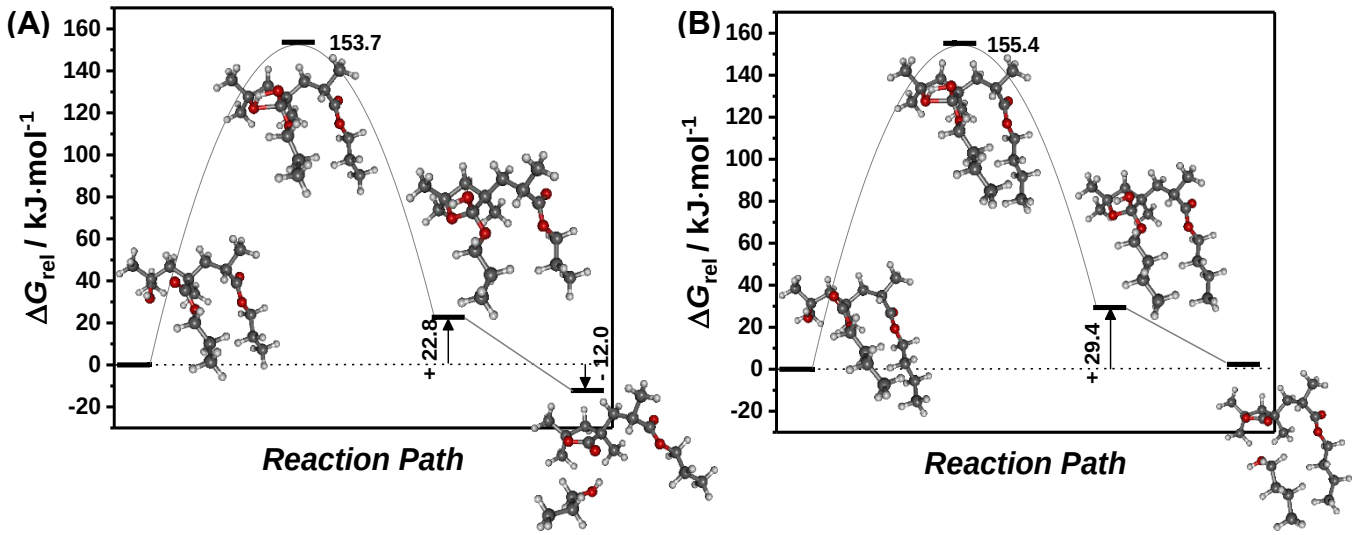

Figure 3 Relative Gibbs Free energies of reaction paths after *si* face attack for propyl (A) and butyl (B) substituted molecules. The relative energy of the lowest open polymer is set to ΔG_{rel} = 0.0 kJ·mol^{-1}. Geometries of the propyl and butyl substituted molecules are provided within the graph.

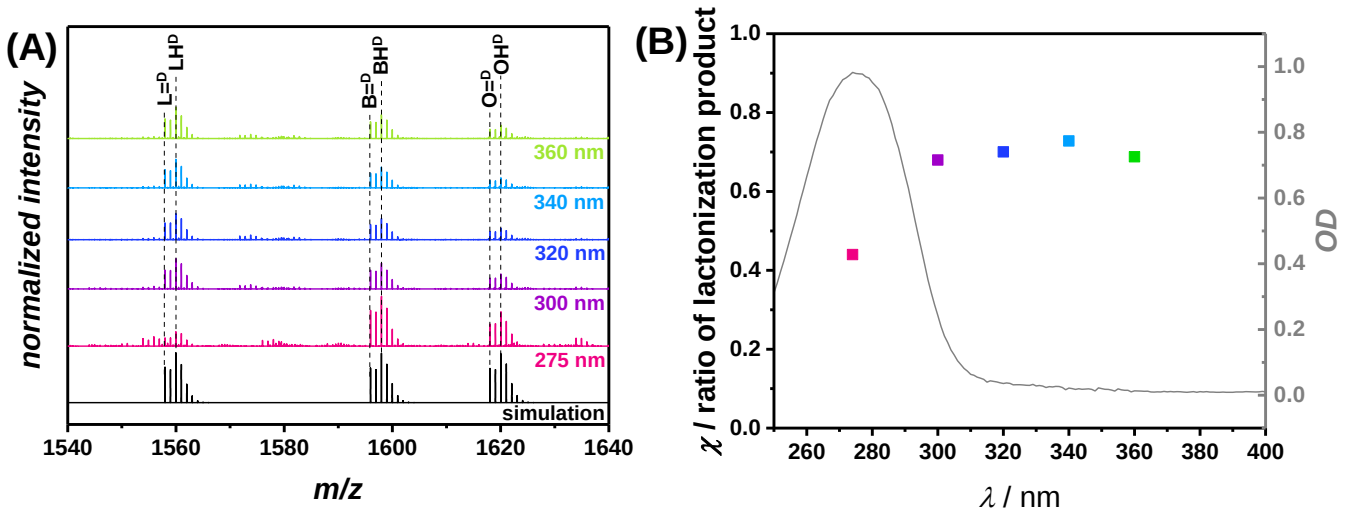

Figure 4 (A) High resolution SEC-ESI mass spectra of the p(*n*PMA) initiated by **Irgacure 2959**, synthesized at low laser energies (0.35 mJ/pulse, 100 Hz, 18 °C, colored spectra) at variable monochromatic wavelengths (275 nm – 360 nm) at a constant photon count and the associated isotopic pattern simulation (black spectrum). (B) Wavelength-dependent transformation of hydroxyl isopropyl to lactone end groups (275 – 360 nm) expressed by the lactonization ratios (shown with the disproportionation product **LH^D**) derived from the peak heights (**OH^D** and **LH^D**; of **Irgacure 2959-p(*n*PMA) (■)**, determined with high resolution SEC-ESI-MS, as well as the UV-Vis spectra of the photoinitiator **Irgacure 2959** in MeOH ($5 \cdot 10^{-5}$ M).

corresponding plots of *E* (0.7-2.5 mJ/pulse) and *T* (0-60°C) for each fragment of **LH^D** vs. the degree of polymerization DP_n, as well as the mass spectra can be found in the Supporting Information (refer to Figure **S19-20** and **Figure S11-12**). As can clearly be seen in **Table S13**- **S14**, the formation of the lactone is not correlated with the employed energy and temperature during PLP.

Conclusions

In summary, we present an in-depth mass spectrometric study of the monomer-, wavelength-, energy and temperature-dependent transformation of hydroxy isopropyl polymer end groups into lactone chain termini. P(MMA), p(EMA), p(*n*PMA), p(*i*PMA), p(*n*BMA), p(*t*BMA), p(DMAEMA), p(BnMA), (initiated by **Irgacure 2959**) were synthesized via PLP at 351 nm, applying low laser energy, as well a constant photon count and subsequently analyzed via SEC-ESI-MS. We demonstrate that the lactonization reaction of the polymer end groups occurs for p(*n*PMA), p(BnMA) and p(DMAEMA). However, the lactonization products could hardly be seen for the polymers p(MMA), p(EMA), p(*i*PMA), p(*n*BMA), and p(*t*BMA). In our DFT calculations, we investigated a direct lactonization with a simple polymer model including 2 monomer units with the most stable all-trans alkyl chains. Factors reducing the high ring closure barrier of the rate-limiting step were not included, e.g. steric effects such as interaction of monomers and conformational flexibility of the alkyl chains, solvent- or monomer-mediated H-transfer, tunneling of the proton through the lactonization barrier. Concluding from our DFT results, there is theoretical evidence that the ester motifs can influence the lactonization and produce thermodynamically more stable lactone products after *si* face attack. The lactonization is not affected by wavelength, energy or temperature and occurs irrespective of these parameters to the same extent. Thus, our study provides an avenue for lactone chain end formation as a function of the monomer based on hydroxy isopropyl-type radical derived end groups. Our findings do not only provide an unexpected end group transformation for one of the most important photoinitiators, but concomitantly an avenue to generate polymers with lactone chain termini by photochemical means.

Conflicts of interest

There are no conflicts to declare.

Acknowledgements

C.B.-K. acknowledges funding for this project from the German Research Council (DFG) as well as the Australian Research Council (ARC) in the form of a Laureate Fellowship enabling his photochemical research program. Long term support by the Queensland University of Technology (QUT) as well as the Karlsruhe Institute of Technology (KIT) in the context of the Science and Technology of Nanosystems (STN) program of the Helmholtz Association are gratefully acknowledged. J.S. PhD studies are partly funded by a Landesgraduierten Stipendium of the state of Baden-Wuerttemberg.

References

1 J. Radebner, A. Eibel, M. Leypold, C. Gorsche, L. Schuh, R. Fischer, A. Torvisco, D. Neshchadin, R. Geier, N. Moszner, R. Liska, G. Gescheidt, M. Haas and H. Stueger, *Angew. Chemie - Int. Ed.*, 2017, **56**, 3103–3107.

2 M. Mitterbauer, M. Haas, H. Stüger, N. Moszner and R. Liska, *Macromol. Mater. Eng.*, 2017, **302**, 1–7.

3 J. Fischer and M. Wegener, *Laser Photonics Rev.*, 2013, **7**, 22–44.

4 M. Kaupp, K. Hiltebrandt, V. Trouillet, P. Mueller, A. S. Quick, M. Wegener and C. Barner-Kowollik, *Chem. Commun.*, 2016, **52**, 1975–1978.

5 K. Hiltebrandt, M. Kaupp, E. Molle, J. P. Menzel, J. P. Blinco and C. Barner-Kowollik, *Chem. Commun.*, 2016, **52**, 9426–9429.

6 B. T. Tuten, J. P. Menzel, K. Pahnke, J. P. Blinco and C. Barner-Kowollik, *Chem. Commun.*, 2017, **53**, 4501–4504.

7 J. P. Menzel, B. B. Noble, A. Lauer, M. L. Coote, J. P. Blinco and C. Barner-Kowollik, *J. Am. Chem. Soc.*, 2017, **139**, 15812–15820.

8 A. Al Mousawi, D. M. Lara, G. Noirbent, F. Dumur, J. Toufaily, T. Hamieh, T. T. Bui, F. Goubard, B. Graff, D. Gigmes, J. P. Fouassier and J. Lalevée, *Macromolecules*, 2017, **50**, 4913–4926.

9 A. M. Pekkanen, R. J. Mondschein, C. B. Williams and T. E. Long, *Biomacromolecules*, 2017, **18**, 2669–2687.

10 C. Decker, *Surf. Coatings Int. Part B Coatings Trans.*, 2005, **88**, 9–17.

11 B.-H. Lee, J.-H. Choi and H.-J. Kim, *J. Coatings Technol. Res.*, 2006, **3**, 221–229.

12 N. Moszner, U. K. Fischer, B. Ganster, R. Liska and V. Rheinberger, *Dent. Mater.*, 2008, **24**, 901–907.

13 B. Richter, V. Hahn, S. Bertels, T. K. Claus, M. Wegener, G. Delaittre, C. Barner-Kowollik and M. Bastmeyer, *Adv. Mater.*, , DOI:10.1002/adma.201604342.

14 Z. W. Wang, X. L. Huang and C. Y. Hu, *Packag. Technol. Sci.*, 2009, **22**, 151–159.

15 X. Zhang, W. Xi, S. Huang, K. Long and C. N. Bowman, *Macromolecules*, 2017, **50**, 5652–5660.

16 A. Beziau, A. Fortney, L. Fu, C. Nishiura, H. Wang, J. Cuthbert, E. Gottlieb, A. C. Balazs, T. Kowalewski and K. Matyjaszewski, *Polym. (United Kingdom)*, 2017, **126**, 224–230.

17 S. Benedikt, J. Wang, M. Markovic, N. Moszner, K. Dietliker, A. Ovsianikov, H. Grützmacher and R. Liska, *J. Polym. Sci. Part A Polym. Chem.*, 2016, **54**, 473–479.

18 A. Eibel, M. Schmallegger, M. Zalibera, A. Huber, Y. Bürkl, H. Grützmacher and G. Gescheidt, *Eur. J. Inorg. Chem.*, 2017, **2017**, 2469–2478.

19 J. Radebner, M. Leypold, A. Eibel, J. Maier, L. Schuh, A. Torvisco, R. Fischer, N. Moszner, G. Gescheidt, H. Stueger and M. Haas, *Organometallics*, 2017, **36**, 3624–3632.

20 P. Jöckle, C. Schweigert, I. Lamparth, N. Moszner, A.-N. Unterreiner and C. Barner-Kowollik, *Macromolecules*, 2017, **50**, 8894–8906.

21 T. N. Eren, N. Okte, F. Morlet-Savary, J. P. Fouassier, J. Lalevee and D. Avci, *J. Polym. Sci. Part A Polym. Chem.*, 2016, **54**, 3370–3378.

22 G. Yilmaz, B. Aydogan, G. Temel, N. Arsu, N. Moszner and Y. Yagci, *Macromolecules*, 2010, **43**, 4520–4526.

23 J. Steinkoenig, M. M. Zieger, H. Mutlu and C. Barner-Kowollik, *Macromolecules*, 2017, **50**, 5385–5391.

24 E. Lee, D. Kim, S. Y. Yang, J.-W. Oh and J. Yoon, *Polym. Chem.*, 2017, **26**, 6786–6794.

25 E. Frick, C. Schweigert, B. B. Noble, H. A. Ernst, A. Lauer, Y. Liang, D. Voll, M. L. Coote, A. N. Unterreiner and C. Barner-Kowollik, *Macromolecules*, 2016, **49**, 80–89.

26 A. Lauer, D. E. Fast, J. Steinkoenig, A. M. Kelterer, G. Gescheidt and C. Barner-Kowollik, *ACS Macro Lett.*, 2017, **6**, 952–958.

27 S. Hurrle, A. Lauer, H. Gliemann, H. Mutlu, C. Wöll, A. S. Goldmann and C. Barner-Kowollik, *Macromol. Rapid Commun.*, 2017, **38**, 1–7.

28 A. Eibel, D. E. Fast, J. Sattelkow, M. Zalibera, J. Wang, A. Huber, G. Müller, D. Neshchadin, K. Dietliker, H. Plank, H. Grützmacher and G. Gescheidt, *Angew. Chemie - Int. Ed.*, 2017, **56**, 14306–14309.

29 R. M. Beesley, C. K. Ingold and J. F. Thorpe, *J. Chem. Soc. Trans.*, 1915, **107**, 1080–1106.

30 S. Huvelle, A. Alouane, T. Le Saux, L. Jullien and F. Schmidt, *Org. Biomol. Chem.*, 2017, **15**, 3435–3443.

31 E. Brenna, F. Distante, F. G. Gatti and G. Gatti, *Catal. Sci. Technol.*, 2017, **7**, 1497–1507.

32 A. Lauer, D. E. Fast, A. M. Kelterer, E. Frick, D. Neshchadin, D. Voll, G. Gescheidt and C. Barner-Kowollik, *Macromolecules*, 2015, **48**, 8451–8460.

33 K. Tang, J. S. Page and R. D. Smith, *J. Am. Soc. Mass Spectrom.*, 2004, **15**, 1416–1423.

34 L. Konermann, E. Ahadi, A. D. Rodriguez and S. Vahidi, 2012.

35 M. A. Zenaidee and W. A. Donald, *Analyst*, 2015, **140**, 1894–1905.

36 H. Fischer and L. Radom, *Angew. Chemie Int. Ed.*, 2001, **40**, 1340–1371.

Table of Content

Installing Lactone Chain Termini During Photoinduced Polymerization